

A Run-to-Run Profile Control Algorithm for Improving the Flatness of Nano-Scale Products

Xin Wang, Su Wu, and Kaibo Wang

Abstract—In scaling-up Carbon Nanotubes (CNTs) array manufacturing, the uniformity of CNTs' height, or flatness of array, is critical for the yield of nanodevices fabricated from CNTs, and thus needs to be properly controlled. However, since the flatness of the CNTs array is better characterized by a profile, the conventional run-to-run (R2R) controllers that are designed for a single or multiple quality indicators are not effective in controlling the CNTs array manufacturing process. Therefore, in this work, we first develop a statistical model to characterize the variation of the flatness profile, and then derive a novel R2R profile controller based on a state-space model and Kalman filter to improve the flatness of CNTs array. The performance of the proposed R2R control algorithm is studied and compared with existing controller via simulation studies.

Note to Practitioners—In the quality control practice, it should be noted that many aggregated quality indicators or the pass/fail conclusions are, in fact, drawn on the basis of complex measurements. Such measurements convey rich information about the process variability and quality patterns, and is therefore critical to quality improvement.

This work focuses on a scaling-up nano-manufacturing process. The quality of the product is characterized by a profile, which contains information about both the location and the flatness of the product. We design a statistical model to characterize product quality, then derive a control algorithm to improve the flatness by adjusting controllable process variables. Such data-driven modeling and control framework is critical to study processes with complex quality metrics and large uncertainties.

Index Terms—Nano-manufacturing, run-to-run (R2R) control, statistical quality control.

I. INTRODUCTION

IN CERTAIN modern manufacturing processes, the product quality is characterized by the flatness of a two-dimensional surface or one-dimensional profile. The flatness reflects the uniformity of some quality variables, usually the thickness or height, over a specified interval. Compared to the traditional univariate or multivariate quality indices, the flatness is usually

formed by the same variable measured at multiple locations on a product surface, or along one or multiple lines on a surface. Therefore, the flatness is a complicated metric that usually convey rich information such as the shape, position, and roughness of a product. To achieve higher product quality, the control of product flatness becomes an important while challenging topic.

In this work, we focus on a real scaling-up nano-manufacturing process for producing Carbon Nanotubes (CNTs) array. CNTs have been considered as a potential candidate to replace a lot of traditional materials due to its excellent photoelectric properties, mechanical strength and flexibility. In 2002, super-aligned CNTs array were first successfully synthesized on silicon wafers using the Chemical Vapor Deposition (CVD) method, which is accomplished in a reaction furnace with flowing gaseous carbon feedstock and argon in the presence of silicon wafer with catalysts [1]. The CVD is essentially a thermal dehydrogenation reaction, whereby the catalyst is utilized to lower the reaction condition required to crack a gaseous hydrocarbon feed into carbon and hydrogen [2]. The resulting CNTs array is well-aligned and formed into bundles by van der Waals force [2]. Continuous and large-scale CNTs films, which have been developed to produce novel products such as touch panels, LCD and other optoelectronic devices, can be easily drawn from the super-aligned CNTs array [3]. Since the first successful experiment in the laboratory, the production of the CNTs array has started to enter the scaling-up stage; factors such as yield, quality and cost are seriously considered to meet high industrial demand [4].

However, due to the immature techniques and limited understanding of the CNTs array synthesis technology, its manufacturing process still suffers from issues such as high cost and low yield, and these are directly dominated by the quality of the CNTs array. In order to have a better understanding for quality of the CNTs array, we briefly introduce how the CNTs array is used for producing thin film, which could be further used to produce touch panels. The CVD synthesis process can produce a forest of tall and super-aligned CNTs, the CNTs array, on a wafer basis, as Fig. 1 shows. First, the CNTs array is cut by laser to remove the edge area (see Fig. 2). Then, the rest of the CNTs array are drawn from one side away from the wafer. Due to the unique adhesion property of the CNTs, a thin-film band is formed naturally (see Fig. 3). The length of the produced thin-film is determined by the height of the CNTs array. The heights of CNTs are measured along a predefined line, termed measuring line, which is perpendicular to drawing direction (see Fig. 2). Fig. 4 shows the height measurement system for CNTs array and heights of the CNTs

Manuscript received June 03, 2013; revised August 28, 2013; accepted September 23, 2013. Date of publication November 07, 2013; date of current version December 31, 2014. This paper was recommended for publication by Associate Editor T. Kawahara and Editor K. Bohringer upon evaluation of the reviewers' comments. The work of K. Wang was supported by the National Natural Science Foundation of China under Grant 71072012, and the Tsinghua University Initiative Scientific Research Program. This work was supported by Prof. S. Fan, Dr. L. Liu, and Dr. Q. Cai from the Tsinghua-Foxconn Nanotechnology Research Center. (*Corresponding author: K. Wang.*)

The authors are with the Department of Industrial Engineering, Tsinghua University, Beijing 100084, China (e-mail: kbwang@tsinghua.edu.cn).

Color versions of one or more of the figures in this paper are available online at <http://ieeexplore.ieee.org>.

Digital Object Identifier 10.1109/TASE.2013.2284935

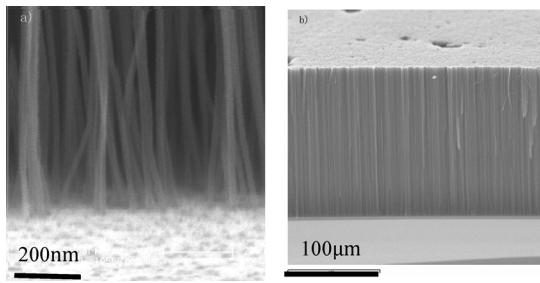


Fig. 1. SEM image of the CNTs array on the silicon wafer in side view.

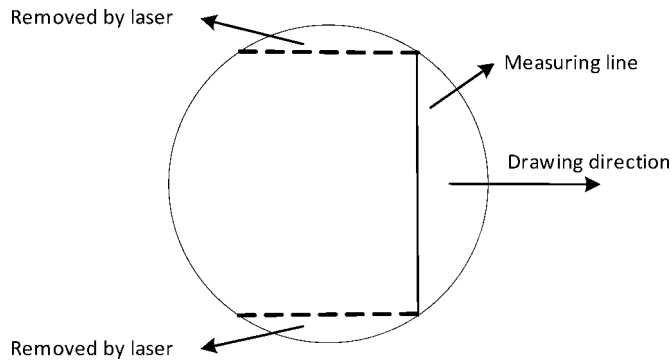


Fig. 2. Schematic drawing of cut lines.

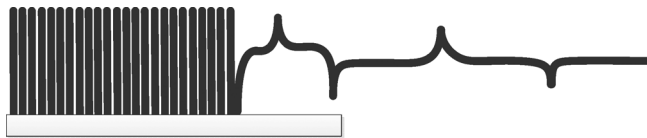


Fig. 3. Illustration of mechanism of transforming CNTs array to film when drawing from one side of the array.

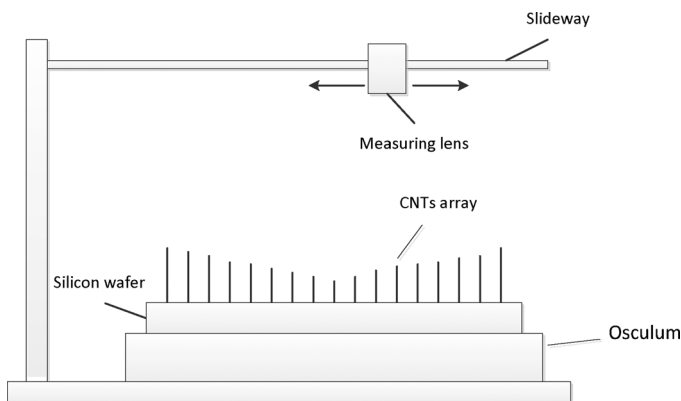


Fig. 4. Side view of the height measurement system and the heights of the CNTs along the measuring line.

along the measuring line on the wafer. During the measurement, the measuring line on the wafer is set to be parallel to the slide way, and the measuring lens can move along the slide way to measure the height of any point on the measuring line. Practically, multiple measurement sites with equal interval are selected for each measuring line.

Due to the mechanism of the CVD process, the height of the CNTs produced on the wafer surface is not ideally uniform. In

practice, height uniformity is desirable for several reasons. First, the wafer with CNTs array is treated using laser beam before entering the drawing stage. The power of the laser beam is determined by the height of the CNTs array. Therefore, if the uniformity of the array is poor, the adjustment of the laser power would be difficult, which may cause damage to the CNTs array if not properly set and incur quality loss. Second, certain electrical properties of the produced film, such as conductivity, is affected by the height of the CNTs array. As uniform conductivity on the film is required, high uniformity of the height is therefore also important. Finally, uneven height distribution cause material wastage. It is observed that CNTs near the center area are usually lower than that near the edge area. Consequently, when drawing the film from the wafer (see Fig. 2), the center area consumes faster than the upper and lower edge area. Thus, high wastage is resulted when the center area has been used up while the upper and lower edge area still has leftover. The amount of leftover is mainly determined by the height uniformity of the CNTs along the direction being parallel to the measuring line. Therefore, controlling the uniformity of the CNTs is an important topic for improving the yield and reducing production cost.

Although the statistical approach has been applied in nanotechnology for recent years, most of the related works mainly focus on design of experiment and process modeling for synthesis [5]–[8], and characterization [9]–[11] of nanomaterial. The process control of nano-manufacturing has not been well studied so far. The CVD process, which is used to produce the CNTs array as introduced above, is a typical run-to-run (R2R) process and widely used in semiconductor manufacturing. In the literature, extensive research has been reported on R2R process control for semiconductor manufacturing [12], [13]. The R2R control, which is a form of discrete control, aims to regulate process output using a filter and a feedback controller. The filter is used to estimate the current system state according to the latest output, and the feedback controller is utilized to determine the new recipe according to the estimated system state.

In the following section, a review of existing work will be given. It will be shown that most existing R2R control algorithms are designed to control one or multiple quality variables. In the aforementioned nano-manufacturing process, the quality objective is to improve the flatness of the CNTs array along a specific direction. As the heights of the CNTs are measured along the measuring line, which has formed a profile naturally, it is equivalent to control the flatness of the profile. However, to the best of our knowledge, very limited work can be found for controlling the flatness of a profile or a surface in R2R control for semiconductor manufacturing and nano-manufacturing. Therefore, in this work, we target to propose a new modeling and run to run profile control method for improving the flatness of the CNTs array.

The rest of this work is organized as follows. Section II presents a review of existing R2R control methods. Section III proposes a new R2R profile control algorithm for the CNTs array production process to improve profile flatness. In Section IV, the performance of the proposed control algorithm is studied using simulation. Finally, Section V concludes this work with suggestions for future research.

II. LITERATURE REVIEW

Ingolfsson and Sach [14] proposed to use exponential weighted moving average (EWMA) statistics to update the estimation of system state (as the filter), this approach is termed EWMA controller, which becomes one of the most popular R2R controllers. The authors also investigated the stability and sensitivity of the EWMA controller under three different disturbances [14]. Bulter and Stefani [15] proposed a double EWMA controller for the process suffered from a drift. Del Castillo [16] discussed the stability and sensitivity of the double EWMA controller. Del Castillo [17] gave a detailed review and analyzed performance of the EWMA controller for process exhibiting dynamics and being influenced by a ARMA noise.

Many manufacturing systems, especially nano-manufacturing, are by nature multiple input and multiple outputs (MIMO) processes [18]. However, the MIMO process cannot be controlled properly by EWMA if there is correlation between different outputs [19]. Tseng *et al.* [18] proposed a multivariate EWMA controller (termed MEWMA) to tackle this problem. The authors also investigated the stability condition and feasible region of this controller, and obtained the discount factor which minimizes the total mean square error (MSE) of process output under assumption that the process disturbance is either a white noise or an IMA time series [18]. Del Castillo *et al.* [19] extended the double EWMA controller to MIMO process. Other methodologies, such as singular value decomposition (SVD) [20] and partial least square (PLS) [21], are also utilized to reduce dimension and decouple the system for MIMO process.

The aforementioned EWMA controller is restricted to the case that the discount factor λ is a predetermined constant. The controller with fixed discount factor usually requires a moderately large number of runs to bring the output to its target [12], [22], and it also cannot minimize the MSE of the estimation unless the process disturbance is IMA noise [23]. Although, several modified EWMA controller with variable discount factor have proposed, these method requires the ratio of the true parameters to the estimated parameter (β/b) [12], [22], which is unrealistic in the CNTs array manufacturing.

Kalman [24] presented a method for recursively estimating states of a linear system based on the most current observation and the past observations. This method, which is known as the Kalman filter, can adjust the Kalman gain adaptively and give the minimization of the MSE among all possible estimators. Therefore, the Kalman filter has the potential to provide a better prediction of system states from the MES point of view. Palmer *et al.* [25] utilized a state space model to describe the photolithography process and Kalman filter to update the state of process. Other researches, such as Del Castillo and Montgomery *et al.* [26], Del Castillo *et al.* [27], Chen *et al.* [28], also illustrated that the Kalman filter can be applied in R2R control.

In all R2R controllers mentioned above, it is assumed that the quality of a process or product can be properly described by a univariate or multivariate quality characteristics. However, in many applications, especially in CNTs array manufacturing (as illustrated in Section I), the quality of a process or product is better represented by a function between the response and one or a set of explanatory variables, which termed profile [29]. The profile can be represented by a linear function [30], non-

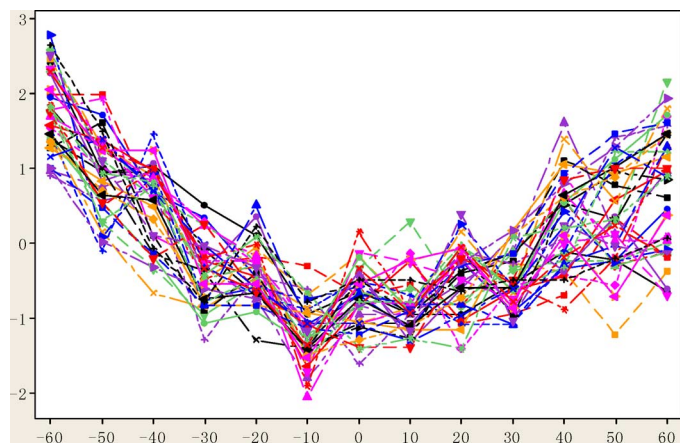


Fig. 5. Profiles of 50 measuring lines (13 measurement sites with interval of 10 mm are selected for each measuring line).

linear function [31], or methods based on wavelets [32], [33] and nonparametric regression [34]; and it has been used to characterize the quality in a lot of applications, such as tonnage signals [35], does response [36], vertical density of wood [37], semiconductor manufacturing [34] and so on. However, most of the researches above related to “profile” focus on the process monitoring and fault detection. Saleh and Rahman [38] utilized the “profile” information of distance between sensor head and wheel metal bond to control the dressing voltage duty ratio for ELID grinding, but their concept of “profile” is a curve derived from raw signal by simple modification, which is not exactly the same as the concept of profile in this paper (see the definition of profile above); in addition, they did not focus on a R2R process control. Therefore, to the best of our knowledge, very limited work has been found for the R2R process control based on profiles.

III. RUN-TO-RUN PROFILE CONTROL FOR CNTs ARRAY MANUFACTURING

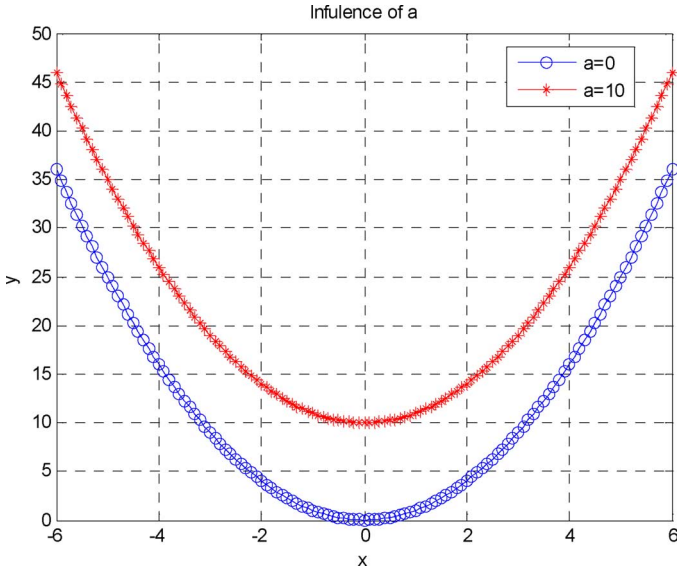
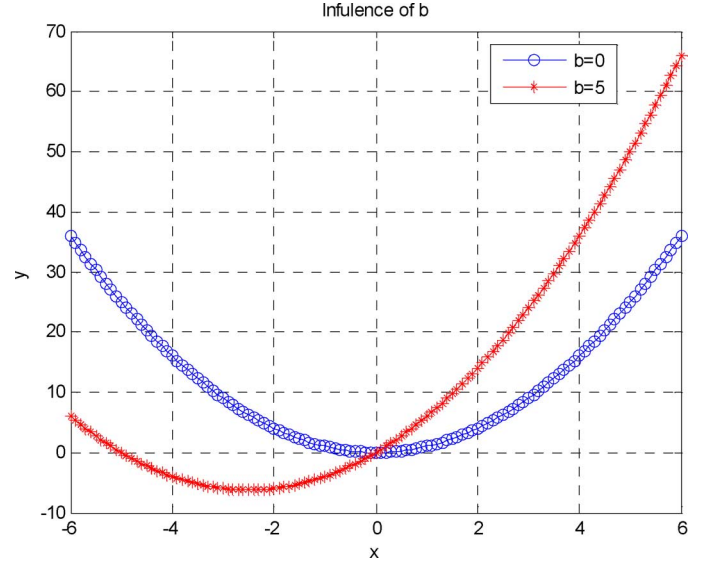
In this section, we first introduce the control objective, and then construct the state-space model for CNTs array production process. After that, the filter and the controller based on the process model are presented, and the stability conditions of the proposed profile controller are discussed at last.

A. Control Objective

It is mentioned above that different from the conventional R2R control, which minimize the deviation of the single or multiple output variables from their respective target values, the control objective for the CNTs array production is defined as the flatness of the measured profile. Fig. 5 presents the profiles obtained from 50 different wafers (after standardization), and it is observed that the height data from different CNTs arrays present similar shape, which can be properly described by a parabola. Hence, we choose the following quadratic function to model the profile:

$$g(x) = a + bx + cx^2. \quad (1)$$

Fitting this equation to the real data proves the adequacy of the model. Profile model in (1) is determined by three param-

Fig. 6. Illustration of effect of parameter a on parabola.Fig. 7. Illustration of effect of parameter b on parabola.

ters defined as $\xi = [a, b, c]^T$, therefore ξ_t is considered as response vector at run t and estimated via least square method as follows:

$$\hat{\xi}_t \equiv [a, b, c]^T = (H^T H)^{-1} H^T Y_t \quad (2)$$

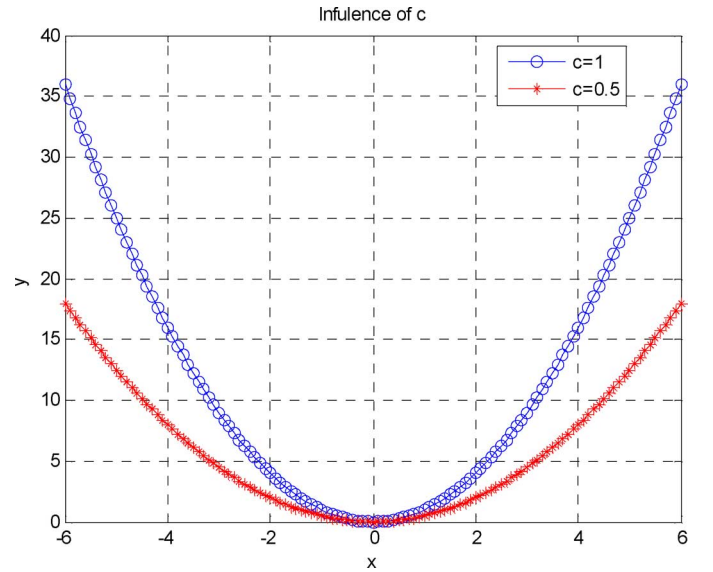
where Y_t is the height vector of the CNTs array produced at run t , H is the matrix defined as follows:

$$H = \begin{bmatrix} 1 & x_1 & x_1^2 \\ 1 & x_2 & x_2^2 \\ \vdots & \vdots & \vdots \\ 1 & x_n & x_n^2 \end{bmatrix} \quad (3)$$

where x_i ($i = 1, 2, \dots, n$) is the coordinate of the i th element of Y_t . Quality characterization using the profile model in (1) has two advantages. First, dimension of the problem can be reduced dramatically while preserving as much information as possible, because the number of measure sites is much larger than 3 in the actual CNTs array production. Second, the profile can filter a part of measurement noise such that performance of the controller can be improved.

The effects of the three parameters on the profile are presented in Figs. 6–8. It can be seen that c has an influence on the curvature of profile (the height difference between boundary sites and central site), b affects the scale of profile (height difference between boundary sites), a mainly determines the absolute height of profile. As it is desirable that the synthesized CNTs along measuring line are uniform and the height of CNTs is approximately equal to prespecified value, the parameters b , c and a are expected to be as close to 0, 0 and the prespecified value as possible. In conclusion, the target T_p of the response vector $\xi = [a, b, c]^T$ is assumed as

$$T_p = \begin{bmatrix} \tau \\ 0 \\ 0 \end{bmatrix}$$

Fig. 8. Illustration of effect of parameter c on parabola.

where τ is the pre-specified height value, the subscript p indicates that it is the target based on profile.

This profile controller aims to minimize the MSE of response vector at run $t + 1$ ($\hat{\xi}_{t+1}$) by choosing a proper process recipe at run t (u_t). Hence, the objective function based on profile is defined as

$$\min_{u_t} f(u_t) = E \left[\left(\hat{\xi}_{t+1} - T_p \right)^T \left(\hat{\xi}_{t+1} - T_p \right) \right] \quad (4)$$

where u_t is the process recipe at run t ($m \times 1$).

It should be noted that in the mechanical design literature, geometric dimensioning and tolerancing (GD&T) has been extensively studied. For example, Kandikjan *et al.* [39] introduced different types of geometric tolerancing scheme, including size, form, orientation, position, run-out and profile. Carr and Ferreora [40] introduced verification models for flatness and

straightness of planar surfaces. In the GD&T system, the requirement for size and flatness are usually assigned separately. However, in process control, as all deviations incur quality loss, the penalties related to size and flatness are reflected in the same objective function. This is consistent with the quality loss function proposed by Taguchi [41] and widely used in the quality control literature [13], [42], [43].

B. Modeling

Although most of the nano-material growth process is complicated and highly nonlinear [5], [8], in CNTs array production, engineers usually restrict the recipes to a very small region in order to prevent unexpected results. Within the small adjustable region, the relationship between the heights of CNTs and the control variables can be approximately described by a linear function according to regression analysis of production data and engineering experience. Therefore, based on our engineering knowledge and verification with real data, we use the following model to characterize the CNTs manufacturing process:

$$Y_{t+1} = A + Bu_t + D_{t+1} \quad (5)$$

where

- Y_{t+1} the height vector with dimension of $k \times 1$;
- A the intercept vector with dimension of $k \times 1$;
- B the slope vector with dimension of $k \times m$;
- D_{t+1} the process disturbance;
- u_t the control vector with dimension of $m \times 1$.

According to the further residual analysis of the production data, the process disturbance D_{t+1} actually consists of two parts, first is the growth noise (N_{t+1}) which can be described and predicted by an ARMA model; second is the measurement error (w_{t+1}) which is usually assumed as white noise and cannot be predicted. The R2R controllers that are based on model in (5), such as MEWMA controller, do not have the ability to differentiate between growth and metrology noise [44]; hence, such kind of controllers treat the process disturbance as an integral whole, regardless of the predictability of the growth noise, when updating the system states. On the contrary, the state-space model, which is divided into a process state equation and output observation equation, has the ability to distinguish two kinds of noise [44]; therefore, it can take advantage of the predictability of the growth noise, which will be illustrated in detail in Section IV. In addition, the state-space model can directly use the Kalman filter, which can minimize the MSE of the estimated system states as introduced in Section II, to update the system states. In addition, this form of modeling strategy has been used to improve the quality and reduce manufacturing cost [45]. Therefore, we try to transform the model in (5) into its state-space representation.

It is shown below that the growth noise (ARMA process) can be characterized by system state transition matrix and covariance matrix in state equation, and measurement error can be characterized by covariance matrix in observation function.

First, it is illustrated that the ARMA (p, q) model can be represented in equivalent state-space form [23]. Consider the ARMA (p, q) process defined by

$$\Phi(L)N_t = \Theta(L)\varepsilon_t \quad (6)$$

where L is the lag operator.

We assume the x_t is the corresponding AR (p) model

$$\Phi(L)x_t = \varepsilon_t. \quad (7)$$

Substitute (7) to (6)

$$\Phi(L)N_t = \Theta(L)\Phi(L)x_t \quad (8)$$

$$N_t = \Theta(L)x_t. \quad (9)$$

Then, we have

$$\begin{cases} N_t = [\theta_{r-1}, \theta_{r-2}, \dots, \theta_0] X_t \\ X_{t+1} = GX_t + E_t \end{cases} \quad (10)$$

where

$$X_t = \begin{bmatrix} x_{t-r+1} \\ x_{t-r+2} \\ \vdots \\ x_t \end{bmatrix}$$

$$G = \begin{bmatrix} 0 & I & 0 & \cdots & 0 \\ 0 & 0 & I & \cdots & 0 \\ \vdots & \vdots & \vdots & \ddots & \vdots \\ 0 & 0 & 0 & \cdots & I \\ \phi_r & \phi_{r-1} & \phi_{r-2} & \cdots & \phi_1 \end{bmatrix}_{(r \times k) \times (r \times k)}$$

$$E_t = \begin{bmatrix} 0 \\ \varepsilon_{t+1} \end{bmatrix}_{[r \times k] \times 1}, \quad \varepsilon_{t+1} \sim N(0, \Sigma)$$

$$r = \max(p, q + 1).$$

According to (10), the state-space representation of model in (5) can be directly obtained as

$$\begin{cases} Y_t = CX_t + w_t \\ X_{t+1} = FX_t + Mu_t + Z_t \end{cases} \quad (11)$$

where $X_t = \begin{bmatrix} Bu_{t-1} \\ X_t \end{bmatrix}$ is the system state vector, $C = [I \quad \Theta]$ is the observation matrix, I is identity matrix

$$\Theta = (\theta_{r-1}, \theta_{r-2}, \dots, \theta_0)_{k \times (k \times r)}$$

$$F = \begin{bmatrix} 0 & 0 \\ 0 & G \end{bmatrix}_{[(r+1) \times k] \times [(r+1) \times k]}$$

is the system state transition matrix, $M = \begin{bmatrix} B \\ 0 \end{bmatrix}_{[(r+1) \times k] \times m}$ is

the process gain, $Z_t = \begin{bmatrix} 0 \\ E_t \end{bmatrix}_{[(r+1) \times k] \times 1}$, Q and R are covariance matrix of w_t and Z_t . It is noted that two kinds of noise are separated in the model in (11).

C. Kalman Filter Based Profile Control Algorithm

After the establishment of process model, a control algorithm based on the model in (11) is required to adjust the CNTs array production properly. The control scheme used to regulate the

process is fundamentally comprised of two parts, which are state updating process and profile based controller respectively. For the first part, it is mentioned above that the Kalman filter can be directly used to update the state for the model in (11) and has ability to provide estimation of system state with minimum MSE; hence, the Kalman filter is utilized to regulate system state in the proposed control algorithm.

The updating process based on the Kalman filter, which is basically divided into two parts (the filtering and prediction respectively), are shown as follows:

$$\text{Prediction : } X_{t+1|t} = FX_{t|t} + Mu_t \quad (12)$$

Minimum prediction
error covariance

$$\text{matrix : } P_{t+1|t} = FP_{t|t}F^T + W \quad (13)$$

$$\text{Kalman gain : } K_t = \frac{P_{t+1|t}C}{Q + C^TP_{t+1|t}C} \quad (14)$$

Filtering :

$$X_{t+1|t+1} = X_{t+1|t} + K_t(Y_{t+1} - CX_{t+1|t}) \quad (15)$$

Minimum filtering error

$$\text{covariance matrix : } P_{t+1|t+1} = (I - K_tC^T)P_{t+1|t}. \quad (16)$$

It is worth noting that the (15) is essentially a weighted sum of state prediction $X_{t+1|t}$ and process innovation $Y_{t+1} - CX_{t+1|t}$, and the weighting value, term Kalman gain, is calculated according to (14). As can be seen, Kalman gain is determined by the relative amount of prediction error, indicated by $P_{t+1|t}$, and measurement error, indicated by Q . If the $P_{t+1|t}$ is comparatively larger, it indicates the measurement result Y_{t+1} is more reliable, and it is reasonable that process innovation $Y_{t+1} - CX_{t+1|t}$ is put larger weight by relatively larger Kalman gain; otherwise, the prediction $X_{t+1|t}$ is more reliable and will be put larger weight by relatively smaller Kalman gain.

For the second part of control scheme, the new recipe is expected to be determined in order to compensate for process disturbance according to system state. It is aforementioned in Section III-A that the objective function based on the profile is shown in (4), and we let the first-order partial derivative of $f(u_t)$ with respect to u_t equal to 0

$$\frac{\partial f(u_t)}{\partial u_t} = 2 \left[(H^T H)^{-1} H^T \hat{B} \right]^T \cdot \left[(H^T H)^{-1} H^T (\hat{B}u_{t+1} + \Theta X_{t+1}) - T_p \right] = 0. \quad (17)$$

The solution to (17) is

$$(H^T H)^{-1} H^T \hat{B}u_t = T_p - (H^T H)^{-1} H^T \Theta \hat{X}_t. \quad (18)$$

The right side of (18) is a vector with dimension of 3 while the dimension of recipe u_t is usually larger than 3 in actual CNTs

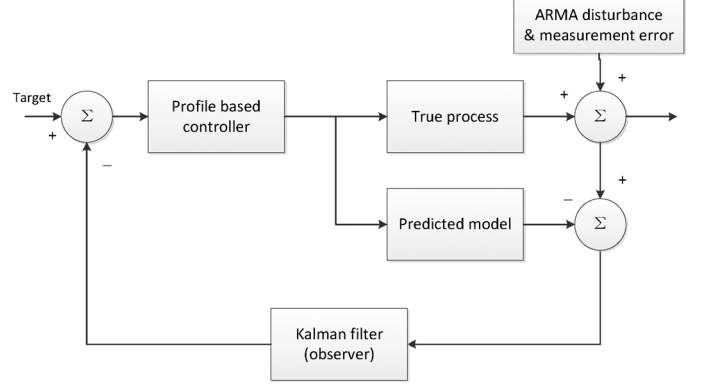


Fig. 9. Schematic diagram of the proposed Kalman-based profile controller.

array production, which means (18) has infinitely many solutions. Under this situation, we want to minimize the adjustment amounts at each run [18], [19], which became the optimization problem as follows:

$$\begin{aligned} \min & (u_t - u_{t-1})^T (u_t - u_{t-1}) \\ \text{s.t.} & (H^T H)^{-1} H^T \hat{B}u_t = \tau - (H^T H)^{-1} H^T \Theta \hat{X}_t. \end{aligned} \quad (19)$$

By using the Lagrange multiplier, the solution is

$$u_t = \left[I - B'(BB')^{-1}B \right] u_{t-1} + B'(BB')^{-1}(T_p - A) \quad (20)$$

where

$$\begin{aligned} A &= (H^T H)^{-1} H^T \Theta \hat{X}_t \\ B &= (H^T H)^{-1} H^T \hat{B}. \end{aligned}$$

Fig. 9 illustrates the proposed profile control loop, which used (12)–(16) to update system states and (20) as controller. In order to discuss the stability condition, we review the proposed control scheme from prospective of linear system theory. It can be seen that the new process recipe u_t is obtained via output feedback controller in (20) according to the system states X_t . However, the system states cannot be directly measured due to lack of physical meaning. An algorithm, termed state observer in linear system theory, is required to reconstruct the system states from latest process output. From this point-of-view, the Kalman filter in the proposed control scheme is equivalent to the state observer in linear system theory. Then, the stability condition is derived as follows.

It is noted that u_{t-1} has been determined and known, so it is supposed to be constant. Hence, if we relax the constraint of u_{t-1} and focus on the general form of the feedback controller, (20) can be expressed as

$$u_t = L\hat{X}_t + v \quad (21)$$

where $L = -B'(BB')^{-1}(H^T H)^{-1}H^T\Theta$, v is the constant term.

Substituting (15) into (11), we get the observer based on the Kalman filter

$$\begin{cases} \hat{X}_{t+1} = (F - FK_tC) \hat{X}_t + FK_tY + Mu_t + Z_t \\ \hat{Y}_t = C\hat{X}_t \end{cases} \quad (22)$$

With the controller in (20) and the observer, the observed system becomes

$$\begin{cases} Y_t = CX_t + w_t \\ X_{t+1} = FX_t + M(L\hat{X}_t + v) + Z_t \\ = FX_t + ML(X_t - \hat{X}_t) + Mv + Z_t \\ = (F + ML)X_t - ML\hat{X}_t + Mv + Z_t \end{cases} \quad (23)$$

where $\tilde{X}_t = X_t - \hat{X}_t$ is the error of observer and its dynamic function is

$$\begin{cases} \tilde{X}_{t+1} = (F - FK_tC) \tilde{X}_t \\ \hat{Y}_t = C\hat{X}_t \end{cases} \quad (24)$$

Hence, \tilde{X}_{t+1} will converge to 0 and the system in (24) will be stable if the eigenvalues of $(F - FK_tC)$ and $(F + ML)$ are within the unite circle.

IV. SIMULATION STUDIES

In this section, we evaluate the performance of the proposed profile controller via simulation study. Traditionally, the engineers characterize the height of the CNTs array as a multivariate vector, and then used the MEWMA controller, as proposed by [18], to adjust the CNTs array production process. Therefore, the MEWMA controller will be used as a benchmark in the following simulation study.

As mentioned before, the manufacturing process of the CNTs array is essentially a CVD process. So the maintenance, cleaning of reacting furnaces and machining aging, which are inevitable after a certain time of production, have a great chance to bring a sudden shift or moderate drift to process output. In addition, the estimation error of model parameters should be also taken into consideration. Hence, in order to illustrate the effectiveness of the proposed profile controller, it will be compared with MEWMA controller under three circumstances, which are ARMA(p, q) noise, ARMA(p, q) with shift and drift, ARMA(p, q) with unknown gain, respectively.

A. Parameters Setting and Criterion

In CNTs array production, there are 15 control variables which affect the height of CNTs array; and 13 measurement sites (as shown in Fig. 10) with interval of 10 mm at a measuring line (from -60 mm to 60 mm) are selected for each CNTs array. Data of more than 200 CNTs arrays/wafers (including both heights and values of the corresponding control variables), gathered from actual production, are utilized to estimate the parameters of the process model.

According to the results of regression, the relationship between process inputs and outputs can be properly described by a linear model with intercept vector shown in Table I and gain matrix shown in Table II. The residual error of the linear model

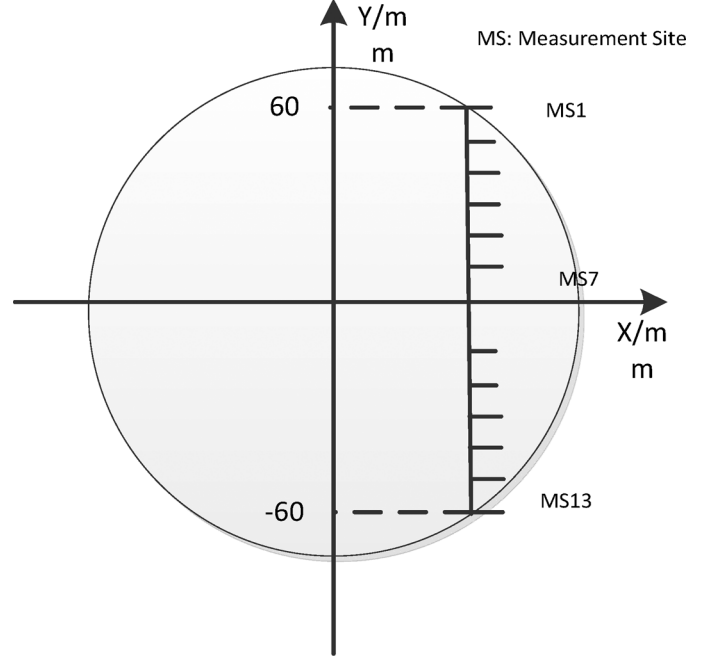


Fig. 10. Illustration of measurement sites.

TABLE I
TRUE VALUES OF INTERCEPT VECTOR

| | | | | | | | |
|--------|--------|--------|--------|--------|--------|--------|--------|
| Number | 1 | 2 | 3 | 4 | 5 | 6 | 7 |
| Slope | 318.88 | 317.01 | 312.83 | 311.86 | 309.15 | 309.61 | 308.17 |
| Number | 8 | 9 | 10 | 11 | 12 | 13 | |
| Slope | 310.44 | 310.52 | 313.69 | 315.45 | 319.44 | 320.97 | |

has been proven to follow a multivariate ARMA (1, 1) model with autoregressive matrix ϕ_1 and moving average matrix θ_1 indicated as Tables III and IV respectively. As we can see, in this case, both autoregressive matrix and moving average matrix is Diagonal matrix, and ε_t follows norm distribution with mean 0 and covariance as Table V, which reveals that the correlation between heights of any two CNTs in the same measuring line is inversely proportional to the distance between them. Measurement system analysis, carried out to estimate the measurement error, illustrates that the measurement error following norm distribution with 0 mean and covariance matrix as a diagonal matrix with diagonal elements of around 5. The above parameters will be considered as the true values in the following simulation studies.

The MEWMA controller is used to compare with the proposed controller as mentioned above. As proposed by Tseng *et al.* [18], its updating equation and control equation are as

$$\hat{A}_t = \lambda(Y_t - Bu_{t-1}) + (1 - \lambda)\hat{A}_{t-1} \quad (25)$$

$$\begin{aligned} u_t = & \left(I - \hat{B}'(\hat{B}\hat{B}')^{-1}\hat{B} \right) u_{t-1} \\ & + \hat{B}'(\hat{B}\hat{B}')^{-1} (T - \hat{A}_t) \end{aligned} \quad (26)$$

TABLE II
TRUE VALUES OF THE GAIN MATRIX

| | | | | | | | | |
|----|-------|--------|--------|---------|--------|--------|---------|-------|
| | 1 | 2 | 3 | 4 | 5 | 6 | 7 | 8 |
| 1 | 0.77 | -8.54 | -7.59 | -12.18 | 32.15 | 111.33 | -109.13 | 39.06 |
| 2 | 0.72 | -7.78 | -7.33 | -11.95 | 33.27 | 116.32 | -113.79 | 38.27 |
| 3 | 0.79 | -7.07 | -7.01 | -11.60 | 32.86 | 115.07 | -112.36 | 37.10 |
| 4 | 0.97 | -7.18 | -6.84 | -11.23 | 32.50 | 113.35 | -110.52 | 37.17 |
| 5 | 0.87 | -7.12 | -6.82 | -10.26 | 31.95 | 111.35 | -108.15 | 35.79 |
| 6 | 0.69 | -7.22 | -6.63 | -10.70 | 30.18 | 103.83 | -101.12 | 35.76 |
| 7 | 0.42 | -7.19 | -6.57 | -11.05 | 31.42 | 109.10 | -106.25 | 34.84 |
| 8 | 0.56 | -7.84 | -6.73 | -11.67 | 29.84 | 101.29 | -99.09 | 33.57 |
| 9 | 0.50 | -8.16 | -6.89 | -11.51 | 29.24 | 99.74 | -97.33 | 34.84 |
| 10 | 0.63 | -8.21 | -7.23 | -11.61 | 30.34 | 103.90 | -101.27 | 35.56 |
| 11 | 0.72 | -8.33 | -7.38 | -12.33 | 28.97 | 98.66 | -95.89 | 35.63 |
| 12 | 0.33 | -9.39 | -7.96 | -12.76 | 29.99 | 102.21 | -99.53 | 34.30 |
| 13 | 0.03 | -9.94 | -8.22 | -13.62 | 26.70 | 87.91 | -85.79 | 33.81 |
| | 9 | 10 | 11 | 12 | 13 | 14 | 15 | |
| 1 | -3.78 | -18.82 | 383.95 | -381.16 | -9.41 | 1.51 | 0.28 | |
| 2 | -1.80 | -20.16 | 413.63 | -411.06 | -9.06 | 1.55 | 0.00 | |
| 3 | -0.02 | -20.96 | 363.06 | -359.67 | -9.48 | 1.59 | -0.29 | |
| 4 | 0.43 | -21.64 | 408.63 | -405.53 | -8.45 | 1.78 | -0.54 | |
| 5 | 2.99 | -23.14 | 382.07 | -378.81 | -7.61 | 1.69 | -0.87 | |
| 6 | 2.81 | -23.07 | 437.86 | -435.00 | -7.10 | 1.67 | -0.91 | |
| 7 | 4.11 | -23.42 | 430.23 | -426.57 | -7.68 | 1.60 | -0.79 | |
| 8 | 4.18 | -22.06 | 382.58 | -378.15 | -9.04 | 1.34 | -0.62 | |
| 9 | 4.71 | -23.68 | 418.91 | -414.93 | -7.97 | 1.54 | -0.93 | |
| 10 | 4.81 | -24.58 | 423.16 | -419.36 | -8.32 | 1.62 | -0.75 | |
| 11 | 3.96 | -23.76 | 412.15 | -407.92 | -9.32 | 1.55 | -0.77 | |
| 12 | 6.01 | -24.42 | 396.94 | -392.10 | -9.74 | 1.28 | -0.77 | |
| 13 | 6.34 | -24.05 | 403.84 | -398.12 | -10.86 | 0.93 | -0.50 | |

TABLE III
AUTOREGRESSIVE MATRIX

| | | | | | | | | | | | | | |
|----|----|----|----|----|----|----|----|----|----|----|----|----|----|
| | 1 | 2 | 3 | 4 | 5 | 6 | 7 | 8 | 9 | 10 | 11 | 12 | 13 |
| 1 | .9 | 0 | 0 | 0 | 0 | 0 | 0 | 0 | 0 | 0 | 0 | 0 | 0 |
| 2 | 0 | .9 | 0 | 0 | 0 | 0 | 0 | 0 | 0 | 0 | 0 | 0 | 0 |
| 3 | 0 | 0 | .9 | 0 | 0 | 0 | 0 | 0 | 0 | 0 | 0 | 0 | 0 |
| 4 | 0 | 0 | 0 | .9 | 0 | 0 | 0 | 0 | 0 | 0 | 0 | 0 | 0 |
| 5 | 0 | 0 | 0 | 0 | .9 | 0 | 0 | 0 | 0 | 0 | 0 | 0 | 0 |
| 6 | 0 | 0 | 0 | 0 | 0 | .9 | 0 | 0 | 0 | 0 | 0 | 0 | 0 |
| 7 | 0 | 0 | 0 | 0 | 0 | 0 | .9 | 0 | 0 | 0 | 0 | 0 | 0 |
| 8 | 0 | 0 | 0 | 0 | 0 | 0 | 0 | .9 | 0 | 0 | 0 | 0 | 0 |
| 9 | 0 | 0 | 0 | 0 | 0 | 0 | 0 | 0 | .9 | 0 | 0 | 0 | 0 |
| 10 | 0 | 0 | 0 | 0 | 0 | 0 | 0 | 0 | 0 | .9 | 0 | 0 | 0 |
| 11 | 0 | 0 | 0 | 0 | 0 | 0 | 0 | 0 | 0 | 0 | .9 | 0 | 0 |
| 12 | 0 | 0 | 0 | 0 | 0 | 0 | 0 | 0 | 0 | 0 | 0 | .9 | 0 |
| 13 | 0 | 0 | 0 | 0 | 0 | 0 | 0 | 0 | 0 | 0 | 0 | 0 | .9 |

TABLE IV
MOVING AVERAGE MATRIX

| | | | | | | | | | | | | | |
|----|----|----|----|----|----|----|----|----|----|----|----|----|----|
| | 1 | 2 | 3 | 4 | 5 | 6 | 7 | 8 | 9 | 10 | 11 | 12 | 13 |
| 1 | .3 | 0 | 0 | 0 | 0 | 0 | 0 | 0 | 0 | 0 | 0 | 0 | 0 |
| 2 | 0 | .3 | 0 | 0 | 0 | 0 | 0 | 0 | 0 | 0 | 0 | 0 | 0 |
| 3 | 0 | 0 | .3 | 0 | 0 | 0 | 0 | 0 | 0 | 0 | 0 | 0 | 0 |
| 4 | 0 | 0 | 0 | .3 | 0 | 0 | 0 | 0 | 0 | 0 | 0 | 0 | 0 |
| 5 | 0 | 0 | 0 | 0 | .3 | 0 | 0 | 0 | 0 | 0 | 0 | 0 | 0 |
| 6 | 0 | 0 | 0 | 0 | 0 | .3 | 0 | 0 | 0 | 0 | 0 | 0 | 0 |
| 7 | 0 | 0 | 0 | 0 | 0 | 0 | .1 | 0 | 0 | 0 | 0 | 0 | 0 |
| 8 | 0 | 0 | 0 | 0 | 0 | 0 | 0 | .1 | 0 | 0 | 0 | 0 | 0 |
| 9 | 0 | 0 | 0 | 0 | 0 | 0 | 0 | 0 | .1 | 0 | 0 | 0 | 0 |
| 10 | 0 | 0 | 0 | 0 | 0 | 0 | 0 | 0 | 0 | .1 | 0 | 0 | 0 |
| 11 | 0 | 0 | 0 | 0 | 0 | 0 | 0 | 0 | 0 | 0 | .1 | 0 | 0 |
| 12 | 0 | 0 | 0 | 0 | 0 | 0 | 0 | 0 | 0 | 0 | 0 | .1 | 0 |
| 13 | 0 | 0 | 0 | 0 | 0 | 0 | 0 | 0 | 0 | 0 | 0 | 0 | .1 |

where \hat{A}_t is the estimated intercept vector from MEWMA algorithm at run t , \hat{B} is the estimated gain matrix, λ is the discount factor ($0 < \lambda < 1$), T is the target vector, of which elements are supposed to be 300 in the following.

The MSE of the heights at measuring line is utilized as criterion to evaluate the performance of two algorithms, and defined as

$$MSE = \frac{1}{N} \sum_{t=1}^N (Y_t - T)^T (Y_t - T) \quad (27)$$

where N is the length of simulation and T is still the target vector.

B. Case One: ARMA (1, 1)

In this case, the proposed profile controller is studied under two situations. First, 500 runs are processed with the proposed profile controller and without any controller respectively, in order to illustrate the effectiveness of our controller. As shown in Figs. 11 and 12, the output converges to target rapidly after a few runs under the Kalman filter-based profile controller even though the initial inputs is chosen improperly, in the contrary,

the output would be totally out of control if no control action is applied. The performance at other points is similar.

Second, we compare the profile controller with the benchmark, which is the MEWMA controller; in order to illustrate our controller is more proper to the CNTs array production process control. Considering that the discount factor λ has a great influence on the performance of MEWMA, the simulation is processed 500 runs for the proposed algorithm and MEWMA with different λ from 0 to 1 (step size is 0.1). As depicted in Fig. 13, the MSE provided by MEWMA with discount factor of 0.5, which performs best among all discount factors, is still larger than MSE delivered by the proposed algorithm. Hence, the proposed profile controller can provide better output than MEWMA.

The reasons for better performance of the Kalman filter-based profile controller lie in three aspects. First, as mentioned above, the state-space model can distinguish between the predictable process noise and the unpredictable measurement noise, while the tradition model considers the process disturbance as one part. Second, based on the state-space model, the Kalman

TABLE V
COVARIANCE MATRIX FOR ε_t

| | 1 | 2 | 3 | 4 | 5 | 6 | 7 |
|----|-------|-------|-------|-------|-------|-------|-------|
| 1 | 5.000 | 4.995 | 4.990 | 4.985 | 4.980 | 4.975 | 4.970 |
| 2 | 4.995 | 5.000 | 4.995 | 4.990 | 4.985 | 4.980 | 4.975 |
| 3 | 4.990 | 4.995 | 5.000 | 4.995 | 4.990 | 4.985 | 4.980 |
| 4 | 4.985 | 4.990 | 4.995 | 5.000 | 4.995 | 4.990 | 4.985 |
| 5 | 4.980 | 4.985 | 4.990 | 4.995 | 5.000 | 4.995 | 4.990 |
| 6 | 4.975 | 4.980 | 4.985 | 4.990 | 4.995 | 5.000 | 4.995 |
| 7 | 4.970 | 4.975 | 4.980 | 4.985 | 4.990 | 4.995 | 5.000 |
| 8 | 4.965 | 4.970 | 4.975 | 4.980 | 4.985 | 4.990 | 4.995 |
| 9 | 4.960 | 4.965 | 4.970 | 4.975 | 4.980 | 4.985 | 4.990 |
| 10 | 4.955 | 4.960 | 4.965 | 4.970 | 4.975 | 4.980 | 4.985 |
| 11 | 4.950 | 4.955 | 4.960 | 4.965 | 4.970 | 4.975 | 4.980 |
| 12 | 4.945 | 4.950 | 4.955 | 4.960 | 4.965 | 4.970 | 4.975 |
| 13 | 4.940 | 4.945 | 4.950 | 4.955 | 4.960 | 4.965 | 4.970 |
| | 8 | 9 | 10 | 11 | 12 | 13 | |
| 1 | 4.965 | 4.960 | 4.955 | 4.950 | 4.945 | 4.940 | |
| 2 | 4.970 | 4.965 | 4.960 | 4.955 | 4.950 | 4.945 | |
| 3 | 4.975 | 4.970 | 4.965 | 4.960 | 4.955 | 4.950 | |
| 4 | 4.980 | 4.975 | 4.970 | 4.965 | 4.960 | 4.955 | |
| 5 | 4.985 | 4.980 | 4.975 | 4.970 | 4.965 | 4.960 | |
| 6 | 4.990 | 4.985 | 4.980 | 4.975 | 4.970 | 4.965 | |
| 7 | 4.995 | 4.990 | 4.985 | 4.980 | 4.975 | 4.970 | |
| 8 | 5.000 | 4.995 | 4.990 | 4.985 | 4.980 | 4.975 | |
| 9 | 4.995 | 5.000 | 4.995 | 4.990 | 4.985 | 4.980 | |
| 10 | 4.990 | 4.995 | 5.000 | 4.995 | 4.990 | 4.985 | |
| 11 | 4.985 | 4.990 | 4.995 | 5.000 | 4.995 | 4.990 | |
| 12 | 4.980 | 4.985 | 4.990 | 4.995 | 5.000 | 4.995 | |
| 13 | 4.975 | 4.980 | 4.985 | 4.990 | 4.995 | 5.000 | |

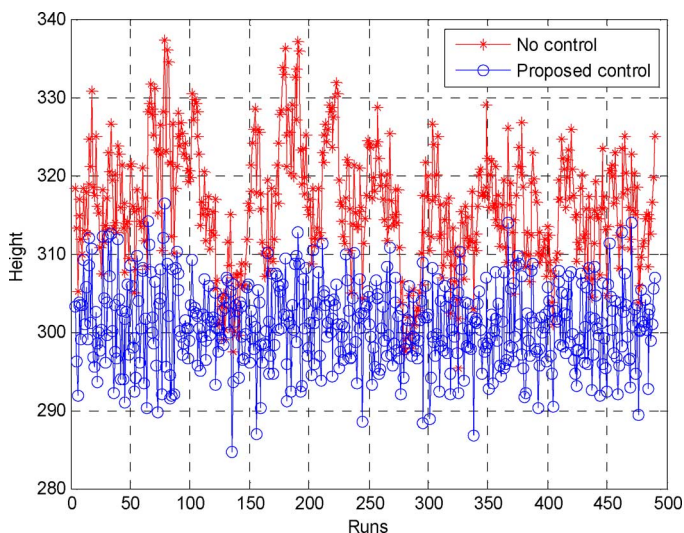


Fig. 11. Performance of the proposed control approach (measurement site 1).

filter use more information, such as auto-regression matrix and moving average matrix, to predict the process disturbance more accurately than MEWMA filter. Last but not the least,

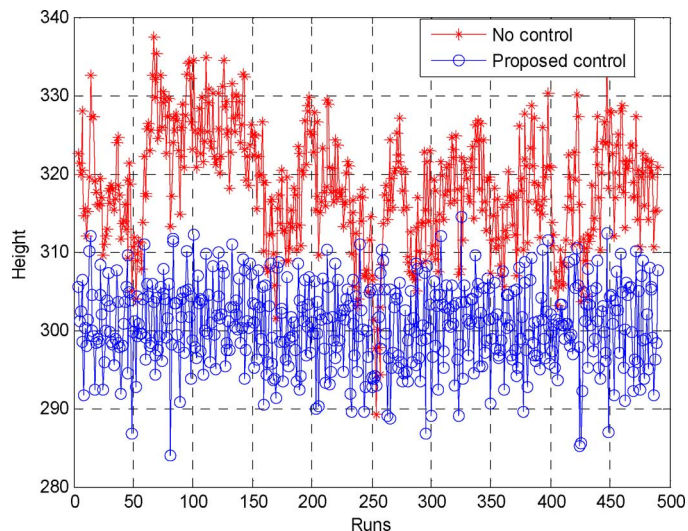


Fig. 12. Performance of the proposed control approach (measurement site 10).

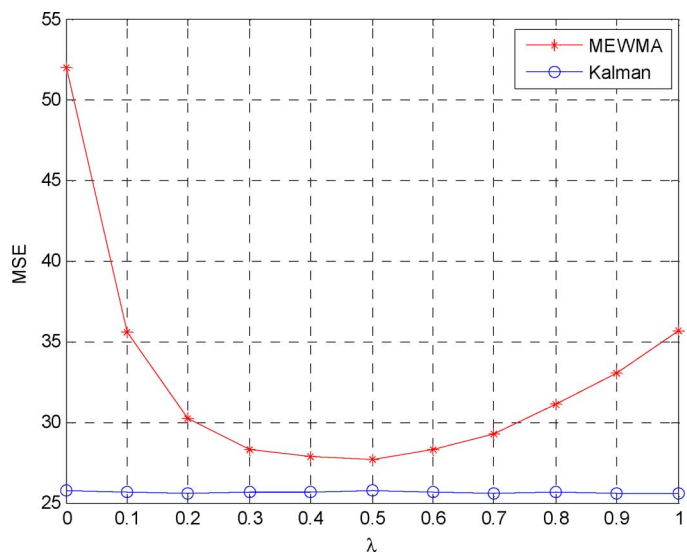


Fig. 13. Comparison between the proposed controller and MEWMA with different discount factors.

quality characterization based on profile can filter a part of measurement noise. All these three reasons make the proposed controller provide lower MSE of the prediction of process disturbance (which is 7.9) than the MEWMA controller (which is 13.1), and then deliver a better control result.

C. Case Two: ARMA (1, 1) With Shift and Drift

If there is a sudden shift with magnitude of d occurring at time k , the true process becomes

$$Y_{t+1} = \begin{cases} A + Bu_t + N_{t+1} + w_{t+1}, & t < k \\ A + Bu_t + N_{t+1} + w_{t+1} + d, & t \geq k \end{cases} \quad (28)$$

In this case, k is assumed to be 0, which means shift occurs at the beginning of the production, shift amount d is set from 0 to 40 with step size of 5 in order to study the effect of d on performance of two algorithms, the other parameters are set the same as Case One. Fig. 14 illustrates that the MSE of output, provided by the Kalman-based profile control approach, increases

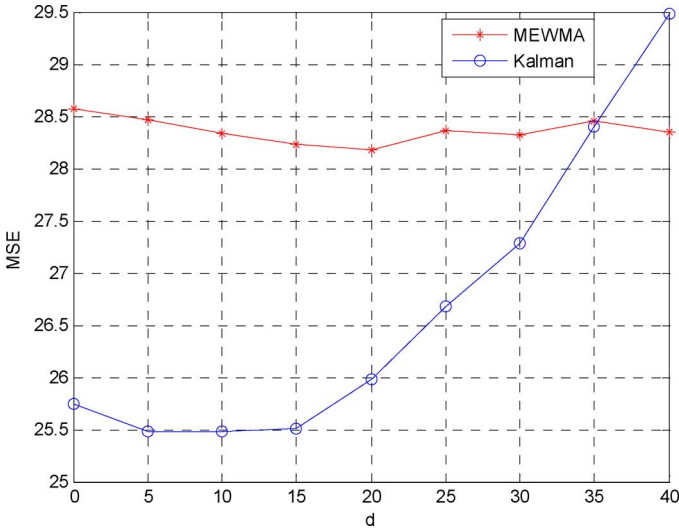


Fig. 14. Comparison between two algorithms under different shift amount.

as the magnitude of the sudden shift; however, the proposed algorithm still can deliver better output if the shift amount is less than a specific value which is approximately 35 in this case. Thus, the proposed algorithm is superior to MEWMA when the magnitude of the shift is moderately small. According to the experience of actual production, the shift amount, caused by maintenance and cleaning of furnace, is usually less than 10% of target value; therefore, the proposed algorithm is more suitable for quality control of CNTs array production than MEWMA.

In addition to sudden shift, the moderate drift should be considered in performance evaluation of control approach. Under this circumstance, the true process becomes

$$Y_{t+1} = A + Bu_t + \delta t + N_{t+1} + w_{t+1} \quad (29)$$

where δ is the drift rate. The two algorithms are compared under different δ from 0 to 0.8 with step size of 0.05. Fig. 15 shows that both of the two control approaches perform worse with the increase of drift rate, however, the proposed method can provide better production outputs than MEWMA if drift rate is less than 0.6.

In conclusion, MSE delivered by the proposed Kalman-based profile control approach is smaller than MEWMA when the shift or drift of process is less than a specific value determined by production process. However, up to now, no evidence has been found to indicate that there is any relatively large shift and drift in the CNTs array manufacturing. Hence, the proposed approach is suitable for process control of the CNTs array manufacturing.

D. Case Three: Unknown Gain

It is mentioned above that the process gain matrix is obtained through regression analysis, which could lead to bias between true process gain and estimated value. Therefore, it is essential to take the estimation bias into consideration when the efficiency of the proposed algorithm is studied; in other words, we should evaluate the performance of the control approach with assumption of unknown gain.

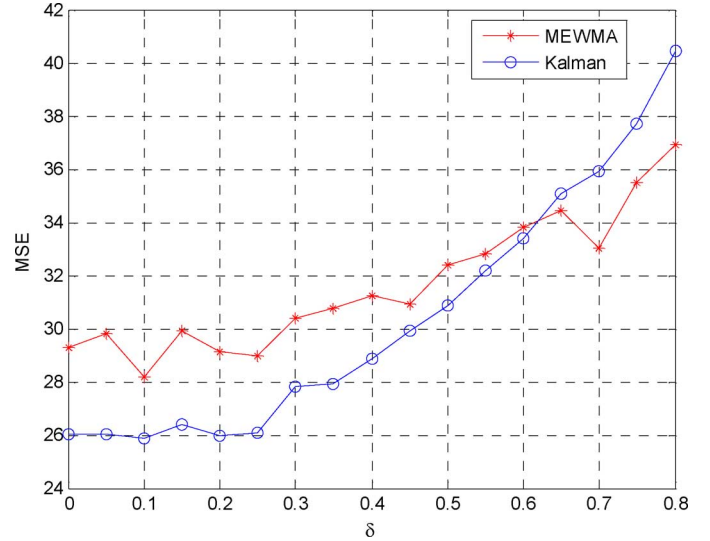


Fig. 15. Comparison between two algorithms under different drift rate.

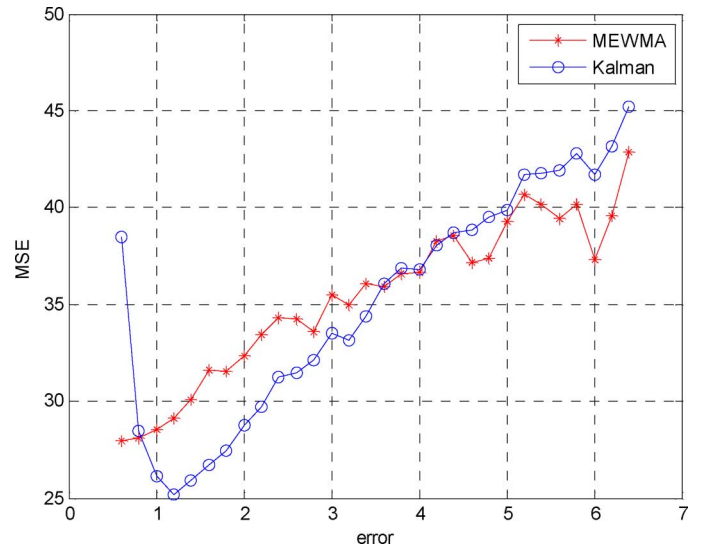


Fig. 16. Comparison between two controllers with unknown gain.

The estimation of the process gain B is assumed to be a linear function of actual value

$$\hat{B} = \zeta B. \quad (30)$$

We compare the MSE of process under two algorithms with ζ from 0.6 to 6.4 with step size of 0.2, because both of two controller will be unstable if ζ is lower than 0.4. The simulation results are depicted in Fig. 16, and the conclusions are as follows.

- 1) As shown in Fig. 16, the proposed profile controller is a little more sensitive to parameter estimation error than MEWMA filter. However, there exists an interval around 1 for parameter estimation error, within which the Kalman filter-based profile controller outperforms the MEWMA controller. In this case, the interval for the estimation error lies in between 0.8 to 3.6. Practically, the ratio of estimated value to the true value of parameters (ζ) is unlikely

larger than 3 if the data collection and analysis method are correct.

- 2) From the long-run point-of-view, it is worth noting that the two sets of algorithm behave in the similar way. When the estimation error is keeping increase, MSE of three parameters under two controllers gradually converges to the same value.

V. CONCLUSION AND FUTURE RESEARCH

The flatness, possessing a great influence on the subsequence processing and macro properties of the produced CNTs film, is considered as a critical quality characteristic of the CNTs array. However, due to the immature technique of the CNTs array synthesis, the flatness of the CNTs array has not been controlled properly. In order to stabilize the process and improve the flatness of CNTs array, a new run to run profile control method is proposed by combining the R2R control technique with the profile characterization of the CNTs array. In this approach, the profile of CNTs array at measurement line is used to construct objective function instead of multivariate vector of height value at each measurement site; state-space model, which has ability to differentiate between process noise and measurement error, is utilized to describe the production process; and Kalman filter is used to update the state of system according to latest output.

The simulation study is carried out to evaluate the performance of the proposed profile controller; three different types of disturbance, namely ARMA (1, 1), ARMA (1, 1) with drift and shift, and ARMA (1, 1) with unknown gain, are considered in the study. The results show that the proposed profile controller has ability to bring output of process to target and outperforms MEWMA under ARMA (1, 1) with and without moderate shift or drift; for the ARMA (1, 1) with unknown gain, there exists an sufficiently large interval around 1 for parameter estimation error in the real application, within which the Kalman filter based profile controller is superior to MEWMA.

Nano-manufacturing is recently beginning to emerge with the development of nanotechnology; a lot of issues related to quality control in nano-manufacturing need to be addressed in the future. First, different types of information, such as expert's opinions and engineering knowledge, should be integrated with experimental data by statistical approach when designing the controller for nano-manufacturing. Second, due to the complex growth mechanism of nanomaterials, modeling for the manufacturing process need to be deeper investigated. Third, quality control theories should be extended to processes with multiple profiles or data-intensive surfaces. The requirement for controlling flatness is also seen in other processes. In this paper, we used a one-dimensional profile to represent the surface. Future research that considers the whole two-dimensional surface data structure may provide better uniformity control across the whole surface. Fourth, measurements that are physically close to each other may be spatially correlated; such spatial correlation is an important feature of complex data and deserves further study. Last but not the least, the proposed profile control is still more sensitive to shift, drift as well as estimation error; hence, it is worth improving its robustness for more broad applications. In addition, it is still a challenge problem that how to model the profile in order to preserve the critical information related to

product quality of interest while filtering as much useless noise as possible, if using profile for process control.

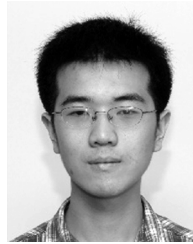
ACKNOWLEDGMENT

The authors thank the associate editor and two anonymous referees for their valuable comments, which have helped us improve this work greatly. They also thank Prof. S. Fan, Dr. L. Liu, and Dr. Q. Cai from Tsinghua-Foxconn Nanotechnology Research Center for providing the raw data, contributing their domain expertise on CNTs array production.

REFERENCES

- [1] K. L. Jiang, Q. Q. Li, and S. S. Fan, "Nanotechnology: Spinning continuous carbon nanotube yarns: Carbon nanotubes weave their way into a range of imaginative macroscopic applications," *Nature*, vol. 419, no. 6909, pp. 801–801, 2002.
- [2] M. Kumar and Y. Ando, "Chemical vapor deposition of carbon nanotubes: A review on growth mechanism and mass production," *J. Nanosci. Nanotechnol.*, vol. 10, no. 6, p. 20, 2010.
- [3] K. Jiang, J. Wang, Q. Li, L. Liu, C. Liu, and S. Fan, "Superaligned carbon nanotube arrays, films, and yarns: A road to applications," *Adv. Mater.*, vol. 23, no. 9, pp. 1154–1161, 2011.
- [4] C. Feng, K. Liu, J.-S. Wu, L. Liu, J.-S. Cheng, Y. Zhang, Y. Sun, Q. Li, S. Fan, and K. Jiang, "Flexible, stretchable, transparent conducting films made from superaligned carbon nanotubes," *Adv. Functional Mater.*, vol. 20, no. 6, pp. 885–891, 2010.
- [5] Q. Huang, "Physics-driven Bayesian hierarchical modeling of the nanowire growth process at each scale," *IIE Trans.*, vol. 43, no. 1, pp. 1–11, 2011.
- [6] Q. Huang, L. Wang, T. Dasgupta, L. Zhu, P. K. Sekhar, S. Bhansali, and Y. An, "Statistical weight kinetics modeling and estimation for silica nanowire growth catalyzed by PD thin film," *IEEE Trans. Autom. Sci. Eng.*, vol. 8, no. 2, pp. 303–310, Apr. 2011.
- [7] L. Wang and Q. Huang, "Cross-domain model building and validation (CDMV): A new modeling strategy to reinforce understanding of nanomanufacturing processes," *IEEE Trans. Autom. Sci. Eng.*, vol. 10, no. 3, pp. 571–578, Jul. 2013.
- [8] T. Dasgupta, C. Ma, V. R. Joseph, Z. L. Wang, and C. F. J. Wu, "Statistical modeling and analysis for robust synthesis of nanostructures," *J. Amer. Statistical Assoc.*, vol. 103, no. 482, pp. 594–603, Jun. 2008.
- [9] X. Deng, V. R. Joseph, W. Mai, Z. L. Wang, and C. J. Wu, "Statistical approach to quantifying the elastic deformation of nanomaterials," *Proc. Nat. Academy Sci.*, vol. 106, no. 29, pp. 11845–11850, 2009.
- [10] L. Xu and Q. Huang, "Modeling the interactions among neighboring nanostructures for local feature characterization and defect detection," *IEEE Trans. Autom. Sci. Eng.*, vol. 9, no. 4, pp. 745–754, Oct. 2012.
- [11] L. Xu and Q. Huang, "EM estimation of nanostructure interactions with incomplete feature measurement and its tailored space filling designs," *IEEE Trans. Autom. Sci. Eng.*, vol. 10, no. 3, pp. 579–587, Jul. 2013.
- [12] S. T. Tseng, F. Tsung, and P. Y. Liu, "Variable EWMA run-to-run controller for drifted processes," *IIE Trans.*, vol. 39, no. 3, pp. 291–301, 2007.
- [13] K. Wang and F. Tsung, "Run-to-run process adjustment using categorical observations," *J. Qual. Technol.*, vol. 39, no. 4, pp. 312–325, 2007.
- [14] A. Ingolfsson and E. Sachs, "Stability and sensitivity of an EWMA controller," *J. Qual. Technol.*, vol. 25, no. 4, pp. 271–287, 1993.
- [15] S. W. Butler and J. A. Stefani, "Supervisory run-to-run control of polysilicon gate etch using in-situ ellipsometry," *IEEE Trans. Semicond. Manuf.*, vol. 7, no. 2, pp. 193–201, 1994.
- [16] E. Del Castillo, "Long run and transient analysis of a double EWMA feedback controller," *IIE Trans.*, vol. 31, no. 12, pp. 1157–1169, 1999.
- [17] E. Del Castillo and A. M. Hurwitz, "Run-to-run process control: Literature review and extensions," *J. Qual. Technol.*, vol. 29, no. 2, pp. 184–196, 1997.
- [18] S. T. Tseng, R. J. Chou, and S. P. Lee, "A study on a multivariate EWMA controller," *IIE Trans.*, vol. 34, no. 6, pp. 541–549, 2002.
- [19] E. Del Castillo and R. Rajagopal, "A multivariate double EWMA process adjustment scheme for drifting processes," *IIE Trans.*, vol. 34, no. 12, pp. 1055–1068, 2002.
- [20] W. Wu and C. Y. Maa, "Double EWMA controller using neural network-based tuning algorithm for MIMO non-squared systems," *J. Process Control*, vol. 21, no. 4, pp. 564–572, 2011.

- [21] J. H. Chen and F. Wang, "PLS based dEWMA run-to-run controller for MIMO non-squared semiconductor processes," *J. Process Control*, vol. 17, no. 4, pp. 309–319, 2007.
- [22] S. T. Tseng, A. B. Yeh, F. Tsung, and Y. Y. Chan, "A study of variable EWMA controller," *IEEE Trans. Semicond. Manuf.*, vol. 16, no. 4, pp. 633–643, 2003.
- [23] G. Box and G. M. Jenkins, *Time Series Analysis Forecasting and Control*. Oakland, CA, USA: Holden-Day, 1976.
- [24] R. E. Kalman, "A new approach to linear filtering," *ASME J. Basic Eng.*, no. 3, pp. 35–45, 1960.
- [25] E. Palmer, W. Ren, C. J. Spanos, and K. Poolla, "Control of photoresist properties: A Kalman filter based approach," *IEEE Trans. Semicond. Manuf.*, vol. 9, no. 2, pp. 208–214, 1996.
- [26] E. Del Castillo and D. C. Montgomery, "A Kalman filtering process-control scheme with an application in semiconductor short-run manufacturing," *Qual. Rel. Eng. Int.*, vol. 11, no. 2, pp. 101–105, 1995.
- [27] E. Del Castillo, R. Pan, and B. M. Colosimo, "A unifying view of some process adjustment methods," *J. Qual. Technol.*, vol. 35, no. 3, pp. 286–293, 2003.
- [28] J. H. Chen, T. W. Kuo, and A. C. Lee, "Run-by-run process control of metal sputter deposition: Combining time series and extended Kalman filter," *IEEE Trans. Semicond. Manuf.*, vol. 20, no. 3, pp. 278–285, Aug. 2007.
- [29] W. H. Woodall, D. J. Spitzner, D. C. Montgomery, and S. Gupta, "Using control charts to monitor process and product quality profiles," *J. Qual. Technol.*, vol. 36, no. 3, pp. 309–320, 2004.
- [30] K. Kim, M. A. Mahmoud, and W. H. Woodall, "On the monitoring of linear profiles," *J. Qual. Technol.*, vol. 35, no. 3, pp. 317–328, 2003.
- [31] J. D. Williams, W. H. Woodall, and J. B. Birch, "Statistical monitoring of nonlinear product and process quality profiles," *Qual. Rel. Eng. Int.*, vol. 23, no. 8, pp. 925–941, 2007.
- [32] J. H. Jin and J. J. Shi, "Automatic feature extraction of waveform signals for in-process diagnostic performance improvement," *J. Intell. Manuf.*, vol. 12, no. 3, pp. 257–268, 2001.
- [33] S. Y. Zhou, B. C. Sun, and J. J. Shi, "An SPC monitoring system for cycle-based waveform signals using Haar transform," *IEEE Trans. Autom. Sci. Eng.*, vol. 3, no. 1, pp. 60–72, Jan. 2006.
- [34] M. M. Gardner, R. S. J. C. G. Lu, J. J. Wortman, B. E. Hornung, H. H. Heinisch, E. A. Rying, S. Rao, and J. C. Davis, "Equipment fault detection using spatial signatures," *IEEE Trans. Compon., Packag., Manuf. Technol., Part C*, vol. 20, no. 4, pp. 295–304, 1997.
- [35] J. H. Jin and J. J. Shi, "Feature-preserving data compression of stamping tonnage information using wavelets," *Technometrics*, vol. 41, no. 4, pp. 327–339, 1999.
- [36] J. D. Williams, J. B. Birch, W. H. Woodall, and N. M. Ferry, "Statistical monitoring of heteroscedastic dose-response profiles from high-throughput screening," *J. Agricultural Biological and Environmental Statist.*, vol. 12, no. 2, pp. 216–235, Jun. 2007.
- [37] T. M. Young, P. M. Winistorfer, and S. Q. Wang, "Multivariate control charts of MDF and OSB vertical density profile attributes," *Forest Products J.*, vol. 49, no. 5, pp. 79–86, May 1999.
- [38] T. Saleh and M. Rahman, "In-process truing for ELID (electrolytic in-process dressing) grinding by pulsewidth control," *IEEE Trans. Autom. Sci. Eng.*, vol. 8, no. 2, pp. 338–346, Apr. 2011.
- [39] T. Kandikjan, J. J. Shah, and J. K. Davidson, "A mechanism for validating dimensioning and tolerancing schemes in CAD systems," *Comput.-Aided Design*, vol. 33, no. 10, pp. 721–737, 2001.
- [40] K. Carr and P. Ferreira, "Verification of form tolerances Part I: Basic issues, flatness, and straightness," *Precision Eng.*, vol. 17, no. 2, pp. 131–143, 1995.
- [41] G. Taguchi, *Introduction to Quality Engineering: Designing Quality Into Products and Processes*. Tokyo, Japan: Asian Productivity Org., 1986.
- [42] F. He, K. Wang, and W. Jiang, "A general harmonic rule controller for run-to-run process control," *IEEE Trans. Semicond. Manuf.*, vol. 22, no. 2, pp. 232–44, May 2009.
- [43] J. Lin and K. Wang, "A Bayesian framework for online parameter estimation and process adjustment using categorical observations," *IIE Trans.*, vol. 44, no. 4, pp. 291–300, 2012.
- [44] W. J. Campbell, S. K. Firth, A. J. Toprac, and T. F. Edgar, "A comparison of run-to-run control algorithms," in *Proc. Amer. Control Conf.*, 2002, vol. 1–6, pp. 2150–2155.
- [45] J. Liu, J. Jin, and J. Shi, "State space modeling for 3-d variation propagation in rigid-body multistage assembly processes," *IEEE Trans. Autom. Sci. Eng.*, vol. 7, no. 2, pp. 274–290, Apr. 2010.



(INFORMS).



Tech. Industrialization.



His research is devoted to statistical quality control and data-driven complex system modeling, monitoring, diagnosis and control, with a special emphasis on the integration of engineering knowledge and statistical theories for solving problems from the real industry.

Dr. Wang is a member of INFORMS, ASQ, and IIE.

Xin Wang received the B.S. degree from the Department of Industrial Engineering, Xi Dian University, Xi'an, China, in 2009. He is currently working towards the Ph.D. degree at the Department of Industrial Engineering, Tsinghua University, Beijing, China.

His general research interests include statistical modeling, process control and experiment design for nano-manufacturing.

Mr. Wang is a Member of Institute for Operations Research and the Management Sciences

Su Wu received the Ph.D. degree in mechanical engineering from the Tsinghua University, Beijing, China in 1994.

He is currently a Professor with the Department of Industrial Engineering, Tsinghua University, Beijing, China. His research focus is on manufacturing and service quality control, manufacturing technology, reliability and maintenance.

Prof. Wu is a member of Editorial Board for the *International Journal of Production Economics*, and an Associate Member of China High

Kaibo Wang received the B.S. and M.S. degrees in mechatronics from Xi'an Jiaotong University, Xi'an, China, and the Ph.D. degree in industrial engineering and engineering management from the Hong Kong University of Science and Technology, Hong Kong.

He is an Associate Professor with the Department of Industrial Engineering, Tsinghua University, Beijing, China. He has published papers in the *Journal of Quality Technology*, the *IIE Transactions*, *Quality and Reliability Engineering International*, the *International Journal of Production Research*, and others.